

## IMPLICATIONS OF GAMMA-RAY TRANSPARENCY CONSTRAINTS IN BLAZARS: MINIMUM DISTANCES AND GAMMA-RAY COLLIMATION

PETER A. BECKER AND MENAS KAFATOS

Center for Earth Observing and Space Research, Institute for Computational Sciences and Informatics, and  
 Department of Physics and Astronomy, George Mason University, Fairfax, VA 22030-4444

Received 1994 August 22; accepted 1995 May 12

### ABSTRACT

We develop a general expression for the  $\gamma - \gamma$  absorption coefficient,  $\alpha_{\gamma\gamma}$ , for  $\gamma$ -rays propagating in an arbitrary direction at an arbitrary point in space above an X-ray-emitting accretion disk. The X-ray intensity is assumed to vary as a power law in energy and radius between the outer disk radius,  $R_0$ , and the inner radius,  $R_{ms}$ , which is the radius of marginal stability for a Schwarzschild black hole. We use our result for  $\alpha_{\gamma\gamma}$  to calculate the  $\gamma - \gamma$  optical depth,  $\tau_{\gamma\gamma}$ , for  $\gamma$ -rays created at height  $z$  and propagating at angle  $\Phi$  relative to the disk axis, and we show that for  $\Phi = 0$  and  $z \gtrsim R_0$ ,  $\tau_{\gamma\gamma} \propto E^\alpha z^{-2\alpha-3}$ , where  $\alpha$  is the X-ray spectral index and  $E$  is the  $\gamma$ -ray energy. As an application, we use our formalism to compute the minimum distance between the central black hole and the site of production of the  $\gamma$ -rays detected by EGRET during the 1991 June flare of 3C 279. In order to obtain an upper limit, we assume that all of the X-rays observed contemporaneously by *Ginga* were emitted by the disk. Our results suggest that the observed  $\gamma$ -rays may have originated within  $\lesssim 45GM/c^2$  from a black hole of mass  $\gtrsim 10^9 M_\odot$ , perhaps in active plasma located above the central funnel of the accretion disk. This raises the possibility of establishing a direct connection between the production of the observed  $\gamma$ -rays and the accretion of material onto the black hole. We also consider the variation of the optical depth as a function of the angle of propagation  $\Phi$ . Our results indicate that the “focusing” of the  $\gamma$ -rays along the disk axis due to pair production is strong enough to explain the observed degree of alignment in blazar sources. If the  $\gamma$ -rays are produced isotropically in  $\gamma$ -ray blazars, then these objects should appear as bright MeV sources when viewed along off-axis lines of sight.

*Subject headings:* accretion, accretion disks — black hole physics — galaxies: active —  
 galaxies: individual (3C 279) — gamma rays: theory — radiative transfer

### 1. INTRODUCTION

Over the past several years, the EGRET instrument on board the *Compton Gamma Ray Observatory* (CGRO) has detected high-energy  $\gamma$ -rays from 44 active galactic nuclei (AGNs), and several of these objects have also been detected at lower energies by COMPTEL and OSSE (Fichtel et al. 1994; Hartman et al. 1992; Hermsen et al. 1993; McNaron-Brown et al. 1994; von Montigny et al. 1995). One of the most dramatic events seen was the intense  $\gamma$ -ray flare of 3C 279 observed in 1991 June, which has called into question the viability of a number of theoretical models for  $\gamma$ -ray emission in AGNs. Most of the energy emitted during the flare appeared at energies exceeding  $\sim 100$  MeV, with an implied (isotropic) luminosity of  $\sim 10^{48}$  ergs  $s^{-1}$ . However, the actual luminosity may have been several orders of magnitude lower if the emission was not isotropic, but rather “focused” onto a small region of the sky due to some alignment mechanism such as relativistic beaming or geometrical collimation. In particular, the hypothesis of relativistic motion is consistent with observations of apparent superluminal motion, flat radio spectra, rapid optical variability and high polarization in blazars.

In addition to beaming and geometrical collimation,  $\gamma - \gamma$  pair production in the X-ray field of the accretion disk could in principle lead to preferential escape of the  $\gamma$ -rays along the symmetry axis of the disk, due to the strong angular dependence of the pair-production cross section. The phenomenon of  $\gamma - \gamma$  “focusing” is related to the more general issue of  $\gamma - \gamma$  transparency, which sets a minimum distance between the central black hole and the site of  $\gamma$ -ray production,  $z_{\gamma\gamma}$ . One usually finds that  $z_{\gamma\gamma}$  greatly exceeds the cooling length,

$$z_{\text{cool}} = cE \left( \left. \frac{dE}{dt} \right|_{\text{synch}} + \left. \frac{dE}{dt} \right|_{\text{IC}} \right)^{-1}, \quad (1.1)$$

for relativistic electrons of energy  $E$  traveling at essentially the speed of light  $c$  and suffering inverse-Compton and synchrotron losses in the intense magnetic and radiation fields close to the center of the active nucleus (Dermer & Schlickeiser 1993). An efficient pair creation and/or reacceleration mechanism is therefore required in order to explain the presence of relativistic electrons sufficiently far from the black hole to produce observable  $\gamma$ -rays. The nature of this mechanism is unclear, and several possibilities have been suggested, including shocks propagating along a jet (Blandford 1993), the decay of charged pions resulting from hadronic collisions (Bednarek 1993), and the acceleration of electrons and positrons via wave-particle interactions in the funnel of a thick accretion disk (Becker, Kafatos, & Maisack 1994). Constraints on the mechanism are provided by estimates of the distance over which it must operate,  $z_{\gamma\gamma} - z_{\text{cool}}$ . Clearly, the closer one can place the  $\gamma$ -ray production site to the black hole while maintaining  $\gamma$ -ray transparency, the easier it will be to power the observed emission using accretion. It is therefore interesting to calculate the minimum distance satisfying the  $\gamma$ -ray transparency constraint in the context of a specific X-ray emission scenario, and that is the focus of this paper.

Gould & Schröder (1967) calculated the absorption coefficient ( $\alpha_{\gamma\gamma} \propto \text{cm}^{-1}$ ) describing the process  $\gamma + \gamma' \rightarrow e^+ + e^-$  for high-energy photons traversing a soft photon gas, and their formalism has been used subsequently by Blandford (1993), Dermer & Schlickeiser (1994), and Bednarek (1993) to estimate the absorption probability for  $\gamma$ -rays traversing the X-ray field of an AGN. The detailed results depend strongly on the energy and angular distribution of the soft radiation and are therefore sensitive to the presence of scattered radiation, which is more isotropic than the primary radiation emitted by the disk. Blandford (1993) and Dermer & Schlickeiser (1994) assumed that the soft photon distribution is isotropic, which is reasonable if the X-ray distribution is dominated by the scattered component. However, the relative importance of the scattered photons compared to the primary (accretion disk) photons is determined by the electron scattering optical depth above the disk, which is not known with any certainty. Bednarek (1993) adopted the opposite viewpoint in his calculation of the optical depth to pair production ( $\tau_{\gamma\gamma}$ ), neglecting electron scattering and instead treating the full anisotropy of the soft radiation field produced by the accretion disk. He assumed a standard disk radiating as a blackbody with local temperature  $T(R) \propto R^{-3/4}$ . The resulting X-ray intensity (integrated over the face of the disk) has the characteristic power-law shape  $I_\nu \propto \nu^{1/3}$  (e.g., Pringle 1981). This is inconsistent with most AGN (and blazar) X-ray spectra (with  $I_\nu \propto \nu^{-1/2}$  typically), which are usually better fitted using hot, two-temperature accretion disk models (e.g., Shapiro, Lightman, & Eardley 1976, hereafter SLE) in the energy range relevant for pair production ( $\epsilon > 261$  eV for  $\gamma$ -ray energy  $E = 1$  GeV; see eq. [3.4]).

In  $\gamma$ -ray loud blazars such as 3C 279, variability arguments suggest that a significant fraction of the observed X-rays are probably produced in a relativistic beam moving toward the observer (Makino et al. 1989). Since these X-rays are co-aligned with the observed high-energy  $\gamma$ -rays, they do not contribute substantially to the  $\gamma - \gamma$  opacity, and therefore they do not strongly constrain the minimum distance between the black hole and the site of  $\gamma$ -ray production. However, as we demonstrate below, an estimate of this distance can be obtained by considering the attenuation of the  $\gamma$ -rays due to collisions with X-rays emitted by an underlying accretion disk. In order to tie the distance estimate we obtain to the multifrequency observations of particular objects such as 3C 279 without creating unnecessary theoretical complexity, in this paper we make the further simplifying assumption that *all* of the contemporaneously observed X-rays were emitted by the accretion disk. By *overestimating* the X-ray flux emitted by the disk, we obtain an “upper limit” on the minimum distance between the black hole and the point of creation of the observed  $\gamma$ -rays, and we expect that a proper accounting for the component of the X-ray flux generated in the relativistic beam would further reduce this distance. In any event, the upper limit we obtain is small enough to allow for the possibility of establishing a direct connection between the production of the observed high-energy  $\gamma$ -rays and the accretion of matter onto the black hole.

## 2. X-RAY INTENSITY OF THE DISK

Electrons in the hot, inner region of a two-temperature accretion disk produce power-law inverse-Compton X-ray emission by upscattering UV radiation produced in the cool (single-temperature) surrounding region. The temperature of the electrons in the hot region is maintained at a nearly uniform value in the range  $T_e \sim 10^9 - 10^{10}$  K by the “Compton thermostat” mechanism (SLE; Eilek & Kafatos 1983, hereafter EK), and the emitted X-ray spectrum has the characteristic power-law shape

$$I_\epsilon \propto \epsilon^{-\alpha}, \quad \alpha = -\frac{3}{2} + \sqrt{\frac{9}{4} + \frac{4}{y}}, \quad (2.1)$$

in the frame of the source, where  $y \equiv (4kT_e/m_e c^2) \text{Max}(\tau_{\text{es}}, \tau_{\text{es}}^2) \sim 1$  is the Compton  $y$ -parameter,  $m_e$  is the electron mass, and  $\tau_{\text{es}}$  is the electron-scattering half-thickness of the disk. The power law extends up to photon energies  $\epsilon \sim kT_e$ , above which the spectrum declines exponentially. Since  $\alpha$  and  $T_e$  are essentially constant in the hot inner region of the disk, it follows that the radial variation of the X-ray intensity follows that of the total flux, given by

$$F(R) = \frac{3}{8\pi} \frac{GM\dot{M}}{R^3} \left[ 1 - \left( \frac{6GM}{c^2 R} \right)^{1/2} \right], \quad (2.2)$$

for a quasi-Keplerian accretion disk around a Schwarzschild black hole of mass  $M$ , where  $\dot{M}$  is the accretion rate (Shakura & Sunyaev 1973). Note that the total flux has a nearly power-law dependence on radius  $F(R) \propto R^{-3}$ , with a sharp cutoff at the radius of marginal stability for circular orbits,  $R_{\text{ms}} = 6R_g$ , where  $R_g \equiv GM/c^2$ .

Based upon equations (2.1) and (2.2), we conclude that the X-ray intensity in the frame of the disk can be represented approximately by

$$I_\epsilon(\epsilon, R) = I_0 \left( \frac{\epsilon}{m_e c^2} \right)^{-\alpha} \left( \frac{R}{R_0} \right)^{-\omega} \quad (\propto \text{ergs s}^{-1} \text{ cm}^{-2} \text{ sr}^{-1} \text{ ergs}^{-1}), \quad (2.3)$$

where  $\alpha$  is given by equation (2.1),  $R_0$  is the outer radius of the two-temperature region, and  $R_{\text{ms}} \leq R \leq R_0$ . According to equation (2.2),  $\omega = 3$  for a two-temperature disk, but we shall leave  $\omega$  as a free parameter so that we can make comparisons with uniformly bright disks, with  $\omega = 0$ . Since it is unclear to what degree electron scattering isotropizes the X-rays above the disk, we follow Bednarek's approach, and neglect the effect of electron scattering on the angular distribution of the X-rays. Our neglect of a scattered X-ray component is in some sense self-consistent, since it turns out that most of the  $\gamma - \gamma$  attenuation occurs very close to the disk, where the X-ray distribution is thought to be dominated by unscattered accretion disk photons (Dermer & Schlickeiser 1994). However, the scattered radiation may attenuate the  $\gamma$ -rays over much larger length scales.

Although the inner region of the disk terminates at the radius of marginal stability, the outer radius  $R_0$  of the two-temperature region is more difficult to quantify because of its dependence on the value (and possible variation) of the viscosity parameter  $\alpha$ , but one typically finds  $30R_g \leq R_0 \leq 100R_g$  (SLE; EK). Most of the photons emitted in the “cool” region beyond radius  $R_0$  are too soft

to produce pairs via collisions with  $\gamma$ -rays of energy  $E \sim 1$  GeV, and therefore the effect of these photons on the  $\gamma - \gamma$  absorption coefficient is negligible.

In order to link our calculation of the  $\gamma - \gamma$  absorption coefficient with the X-ray and  $\gamma$ -ray data, we must express the disk-frame intensity parameter  $I_0$  in equation (2.3) in terms of the parameter  $F'_0$  characterizing the observed (cosmologically Doppler-shifted) X-ray flux,

$$F'_i = F'_0 \left( \frac{\epsilon'}{m_e c^2} \right)^{-\alpha} \quad (\propto \text{s}^{-1} \text{ cm}^{-2}), \quad (2.4)$$

which is related to the observed intensity

$$I'_i(\epsilon', R) = I'_0 \left( \frac{\epsilon'}{m_e c^2} \right)^{-\alpha} \left( \frac{R}{R_g} \right)^{-\omega}, \quad (2.5)$$

by

$$F'_i = \int I'_i \cos \theta' d\Omega', \quad (2.6)$$

where primes denote quantities measured in the frame of the Earth.

Since we are mainly interested in blazar sources, where we are presumably viewing the accretion disks face-on, we can express  $F'_0$  in terms of  $I'_0$  and the luminosity distance to the source  $D$  by substituting for the intensity in equation (2.6) using equation (2.5) and integrating over the face of the disk. Making the substitutions  $d\Omega' = 2\pi \sin \theta' d\theta'$  and  $\tan \theta' = R/D$  yields

$$F'_0 = 2\pi D^2 I'_0 \int_{R_{\text{ms}}}^{R_0} \left( \frac{R}{R_g} \right)^{-\omega} \frac{R dR}{(R^2 + D^2)^2}, \quad (2.7)$$

or, in the limit  $D \gg R_0$ ,

$$F'_0 = \frac{2\pi I'_0}{2 - \omega} \left( \frac{D}{R_g} \right)^{-2} \left[ \left( \frac{R_0}{R_g} \right)^{2-\omega} - \left( \frac{R_{\text{ms}}}{R_g} \right)^{2-\omega} \right] \quad (2.8)$$

for  $\omega \neq 2$ , where  $I'_0$  is related to  $I_0$  via the Lorentz transformation of the intensity, which gives for a source located at redshift  $\mathcal{Z}$  (e.g., Begelman, Blandford, & Rees 1984)

$$I'_0 = (1 + \mathcal{Z})^{-3-\alpha} I_0. \quad (2.9)$$

In § 3 we obtain a general formula for the  $\gamma - \gamma$  absorption coefficient for  $\gamma$ -rays propagating above an accretion disk radiating with the X-ray intensity distribution given by equation (2.3).

### 3. PHOTON-PHOTON PAIR PRODUCTION

The exact cross section for  $\gamma - \gamma$  pair production is given by the well-known result (e.g., Jauch & Rohrlich 1955),

$$\sigma_{\gamma\gamma}(\beta) = \frac{3}{16} \sigma_{\text{T}}(1 - \beta^2) \left[ (3 - \beta^4) \ln \left( \frac{1 + \beta}{1 - \beta} \right) - 2\beta(2 - \beta^2) \right], \quad (3.1)$$

where  $\beta$  is the velocity of the positron (or electron) in the center-of-momentum (CM) frame in units of  $c$ , and  $\sigma_{\text{T}}$  is the Thomson cross section. The Lorentz factor of the particles in the CM frame,  $\Gamma$ , is related to the energy of the soft photon  $\epsilon$ , the energy of the  $\gamma$ -ray  $E$ , and the interaction angle between the photon trajectories  $\theta$  by

$$\Gamma^2 = \frac{1}{1 - \beta^2} = \frac{\epsilon E (1 - \cos \theta)}{2m_e^2 c^4}, \quad (3.2)$$

where  $\epsilon$ ,  $E$ , and  $\theta$  are all measured in the same (arbitrary) frame. The cross section for the process,  $\sigma_{\gamma\gamma}$ , vanishes as  $\Gamma \rightarrow 1$ . Hence for fixed  $\epsilon$  and  $E$ , the absorption probability decreases as  $\theta \rightarrow 0$ , and consequently the optical depth to pair production ( $\tau_{\gamma\gamma}$ ) drops sharply as the photons become co-aligned. We therefore anticipate that the value of  $\tau_{\gamma\gamma}$  will depend sensitively on the angular distribution of the soft radiation relative to the direction of propagation of the  $\gamma$ -ray.

#### 3.1. $\gamma - \gamma$ Absorption Coefficient

Working in terms of the specific intensity  $I_\epsilon$ , we can write the differential contribution to the absorption coefficient  $\alpha_{\gamma\gamma}$  due to soft photons propagating in energy range  $d\epsilon$  and in directional range  $d\Omega$  as

$$d\alpha_{\gamma\gamma} = \frac{I_\epsilon}{c\epsilon} \sigma_{\gamma\gamma}(\beta) (1 - \cos \theta) d\epsilon d\Omega. \quad (3.3)$$

We assume that the X-ray intensity of the disk is given by equation (2.3), and that any change in the X-ray spectral index  $\alpha$  occurs below the minimum soft-photon energy required to produce a pair with  $\Gamma = 1$ ,

$$\epsilon_{\min}(\theta) = \frac{2m_e^2 c^4}{E(1 - \cos \theta)} \tag{3.4}$$

Taking  $E = 1$  GeV, we find that  $\epsilon_{\min} = 0.522$  keV for a right-angle collision ( $\cos \theta = 0$ ), and  $\epsilon_{\min} = 0.261$  keV for a head-on collision ( $\cos \theta = -1$ ), which is the minimum possible X-ray energy resulting in pair production. The X-ray spectrum given by equation (2.3) would conflict with the measured EGRET spectrum if extended to arbitrarily high energies, and consequently a break must exist in the energy range 0.1–1 GeV. However, for our purposes, the X-ray power law can formally be extended to infinite energy without producing numerical divergence because  $\sigma_{\gamma\gamma} \propto \epsilon^{-1} \ln \epsilon$  as  $\epsilon \rightarrow \infty$  for fixed  $E$  and  $\theta$ .

Using equation (2.3) for the intensity, integration of equation (3.3) over  $\epsilon$  and  $\Omega$  yields for the absorption coefficient

$$\alpha_{\gamma\gamma} = \frac{I_0}{m_e c^3} \iint_{\epsilon_{\min}(\theta)}^{\infty} \left(\frac{\epsilon}{m_e c^2}\right)^{-1-\alpha} \left(\frac{R}{R_g}\right)^{-\omega} \sigma_{\gamma\gamma}(\beta)(1 - \cos \theta) d\epsilon d\Omega, \tag{3.5}$$

where  $\theta$  is the angle between  $d\Omega$  and the direction of propagation of the  $\gamma$ -ray, and the domain for the  $\Omega$  integration corresponds to the range of solid angles subtended by the disk. Equation (3.5) can be broken into two separate integrals by transforming from  $\epsilon$  to  $\beta$  using equation (3.2). The result is

$$\alpha_{\gamma\gamma} = \frac{I_0}{c} \left(\frac{E}{2m_e c^2}\right)^\alpha \sigma_T \Psi(\alpha) \int (1 - \cos \theta)^{\alpha+1} \left(\frac{R}{R_g}\right)^{-\omega} d\Omega, \tag{3.6}$$

where the integration over  $\beta$  is expressed by the function

$$\Psi(\alpha) \equiv \sigma_T^{-1} \int_0^1 2\beta(1 - \beta^2)^{\alpha-1} \sigma_{\gamma\gamma}(\beta) d\beta, \tag{3.7}$$

plotted in Figure 1.

Equation (3.6) can be used to calculate the absorption coefficient for a  $\gamma$ -ray propagating in an *arbitrary* direction at an *arbitrary* point in space. However, it is sufficient for our purposes to consider  $\gamma$ -rays propagating in a plane that includes the symmetry axis of the disk. Referring to the geometry indicated schematically in Figure 2, we assume that the  $\gamma$ -ray propagates in the  $(x, z)$  plane, where the  $z$ -axis is the symmetry axis of the disk, and we set the azimuthal angle  $\varphi = 0$  along the  $x$ -axis. In general, we wish to relate  $d\Omega$  to the differential area in the disk  $dA = R dR d\varphi$  using

$$d\Omega = \frac{\cos \eta R dR d\varphi}{l^2}, \tag{3.8}$$

where  $\eta$  is the angle between the X-ray trajectory and the normal to the disk surface, and  $l$  is the distance between the photon-photon interaction point and the X-ray emission point in the disk. Representing the location of the  $\gamma$ -ray using polar angle  $\delta$  and distance from the origin  $\rho$ , and assuming that the  $\gamma$ -ray trajectory makes an angle  $\Phi$  with the  $z$ -axis (see Fig. 2), our expression for the

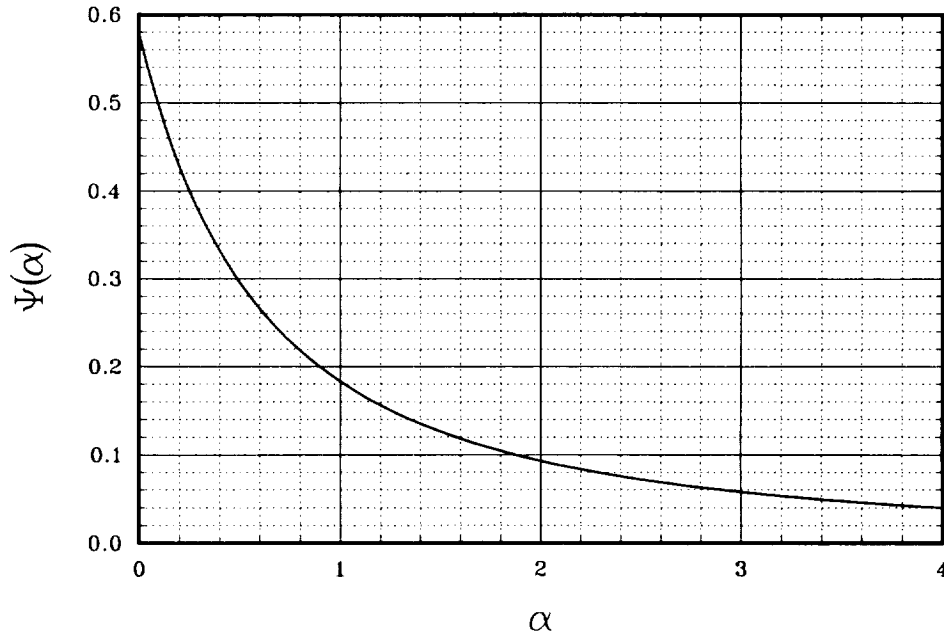


FIG. 1.—The cross section integral function  $\Psi(\alpha)$  (eq. [3.7]). For the 3C 279 data,  $\alpha = 0.68$  (see Makino et al. 1993), and  $\Psi = 0.245$ .

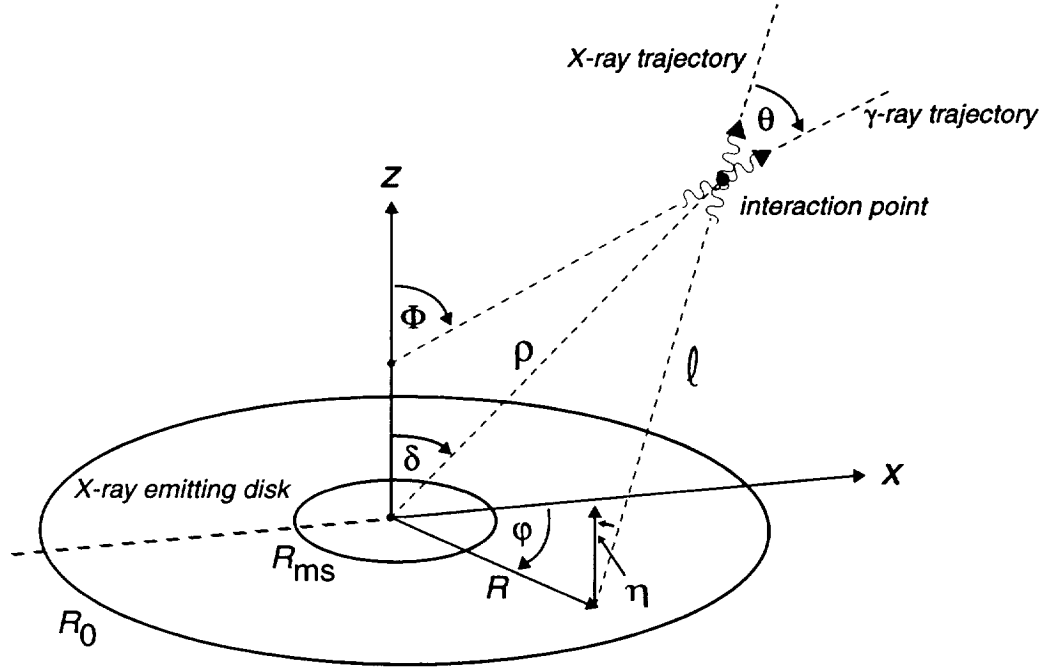


FIG. 2.—Schematic representation of the  $\gamma$ -ray propagation geometry. The  $\gamma$ -ray is located at distance  $\rho$  from the origin and polar angle  $\delta$  and propagates in a plane that includes the  $z$ -axis. Attenuation of the  $\gamma$ -rays occurs as a result of collisions with X-rays generated at all points on the disk. The interaction angle between the photons is  $\theta$ , and the angle between the  $\gamma$ -ray trajectory and the  $z$ -axis is  $\Phi$ .

absorption coefficient becomes

$$\alpha_{\gamma\gamma}(E, \rho, \delta, \Phi) = \frac{I_0}{c} \left( \frac{E}{2m_e c^2} \right)^\alpha \sigma_T \Psi(\alpha) \int_{R_{ms}}^{R_0} \int_0^{2\pi} (1 - \cos \theta)^{\alpha+1} \left( \frac{R}{R_\rho} \right)^{-\omega} \frac{\cos \eta d\varphi R dR}{l^2}, \quad (3.9)$$

where

$$l^2 = \rho^2 + R^2 - 2\rho R \sin \delta \cos \varphi, \quad \cos \theta = \frac{\rho \cos(\delta - \Phi) - R \cos \varphi \sin \Phi}{l}, \quad \cos \eta = \frac{\rho \cos \delta}{l}. \quad (3.10)$$

Note that  $\alpha_{\gamma\gamma} \propto E^\alpha$ , which verifies that softer X-ray spectra yield larger optical depths. Equations (3.9) and (3.10) comprise our fundamental result for the  $\gamma - \gamma$  absorption coefficient for a  $\gamma$ -ray of energy  $E$  propagating in the power-law X-ray field of an accretion disk.

### 3.2. Absorption Coefficient for Propagation along the Disk Axis

One of the most interesting cases to consider is that of the attenuation of  $\gamma$ -rays propagating along the symmetry axis of the disk, since this scenario is of direct relevance for the interpretation of the  $\gamma$ -rays detected by EGRET from blazar sources. In this case equation (3.9) is simplified substantially due to the cylindrical symmetry, and the integration over  $\varphi$  is trivial. We can obtain the absorption coefficient for a  $\gamma$ -ray of energy  $E$  propagating outward along the symmetry axis at height  $z$  by setting  $\rho = z$  and  $\delta = \Phi = 0$  in equation (3.9) and transforming from  $R$  to  $\theta$  using  $\tan \theta = R/z$ , yielding

$$\alpha_{\gamma\gamma}(E, z) = \frac{2\pi I_0}{c} \left( \frac{E}{2m_e c^2} \right)^\alpha \sigma_T \Psi(\alpha) \left( \frac{z}{R_g} \right)^{-\omega} \int_{\theta_{\min}(z)}^{\theta_{\max}(z)} (1 - \cos \theta)^{\alpha+1} \tan^{-\omega} \theta \sin \theta d\theta, \quad (3.11)$$

where  $\theta_{\max}(z)$  [ $\theta_{\min}(z)$ ] is the maximum (minimum) value of the interaction angle  $\theta$  at height  $z$ . Neglecting gravitational curvature of the photon trajectories, we have

$$\cos \theta_{\max}(z) = \frac{z}{\sqrt{z^2 + R_0^2}}, \quad \cos \theta_{\min}(z) = \frac{z}{\sqrt{z^2 + R_{ms}^2}}. \quad (3.12)$$

By writing equation (3.11), we have implicitly assumed that  $z \gg h$ , where  $h$  is the half-thickness of the disk. This condition is trivially satisfied for a thin disk, but the disk may also be considered to be thick, so long as we confine our attention to points sufficiently far above the surface.

## 4. CALCULATION OF THE OPTICAL DEPTH

We can use equations (3.9) and (3.10) to calculate the  $\gamma - \gamma$  optical depth  $\tau_{\gamma\gamma}$  for a  $\gamma$ -ray of energy  $E$  created at radius  $R$  and height  $z$  and propagating at angle  $\Phi$  with respect to the  $z$ -axis by writing

$$\tau_{\gamma\gamma}(E, R, z, \Phi) = \int_0^\infty \alpha_{\gamma\gamma}(E, \rho, \delta, \Phi) d\lambda, \quad (4.1)$$

where  $\lambda$  is the distance traversed by the  $\gamma$ -ray since its creation, and  $\rho$  and  $\delta$  are given by

$$\rho^2 = R^2 + z^2 + \lambda^2 + 2\lambda(R \sin \Phi + z \cos \Phi), \quad \sin \delta = \frac{R + \lambda \sin \Phi}{\rho}, \quad \cos \delta = \frac{z + \lambda \cos \Phi}{\rho}. \quad (4.2)$$

In keeping with equation (3.9), we have assumed that the plane of propagation of the  $\gamma$ -ray includes the  $z$ -axis.

## 4.1. Propagation along the Disk Axis

We can obtain some further simplification for  $\gamma$ -rays propagating along the  $z$ -axis, since then  $\delta = \Phi = R = 0$ , and  $\rho = z + \lambda$ . The optical depth to pair production for a  $\gamma$ -ray of energy  $E$  created at height  $z$  above the center of the disk and propagating outward along the  $z$ -axis is then given by

$$\tau_{\gamma\gamma}(E, z) = \int_z^\infty \alpha_{\gamma\gamma}(E, z_*) dz_*, \quad (4.3)$$

where  $\alpha_{\gamma\gamma}$  is given by equation (3.11). Unfortunately, one must resort to multidimensional numerical integration to compute  $\tau_{\gamma\gamma}$  even in this highly symmetrical case. However, it is possible to obtain a closed-form expression for  $\tau_{\gamma\gamma}$  if  $z \gtrsim R_0$ . Approximating the angular integral in equation (3.11) yields for the absorption coefficient

$$\alpha_{\gamma\gamma}(E, z) \cong A \left( \frac{z}{R_g} \right)^{-2\alpha-4} \left( \frac{E}{4m_e c^2} \right)^\alpha, \quad (4.4)$$

where

$$A \equiv \frac{\pi I_0 \sigma_T \Psi(\alpha)}{(2\alpha + 4 - \omega)c} \left[ \left( \frac{R_0}{R_g} \right)^{2\alpha+4-\omega} - \left( \frac{R_{ms}}{R_g} \right)^{2\alpha+4-\omega} \right]. \quad (4.5)$$

Substituting equation (4.4) into equation (4.3) then yields the approximate far-field solution for the optical depth

$$\tau_{\gamma\gamma}(E, z) \cong \frac{AR_g}{2\alpha + 3} \left( \frac{z}{R_g} \right)^{-2\alpha-3} \left( \frac{E}{4m_e c^2} \right)^\alpha, \quad (4.6)$$

valid if  $z \gtrsim R_0$ . In § 5 we use this result to estimate the height of the  $\gamma$ -ray “photosphere,” defined as the value of  $z$  such that  $\tau_{\gamma\gamma} = 1$ . We also calculate the  $\gamma - \gamma$  optical depth for the  $\gamma$ -ray blazar 3C 279 by focusing on three illustrative scenarios for the propagation of the  $\gamma$ -ray: (i) propagation along the disk axis; (ii) propagation along a line intersecting the disk axis; and (iii) propagation parallel to the disk axis.

## 5. APPLICATION TO 3C 279

The observations of strong fluxes of X-rays and high-energy  $\gamma$ -rays from the blazar 3C 279 in 1991 June allows us to place constraints on the location of the  $\gamma$ -ray emission site based on  $\gamma - \gamma$  transparency requirements. Under the assumption that the contemporaneously observed X-rays were produced by a two-temperature accretion disk, we can use the expressions developed in §§ 3 and 4 to calculate the optical depth traversed by the observed high-energy  $\gamma$ -rays. Since variability arguments (Makino et al. 1989) suggest that a significant fraction of the X-rays were probably produced in a relativistic jet, the results we will obtain for the optical depth  $\tau_{\gamma\gamma}$  are upper limits.

The X-ray flux reported by Makino et al. (1993; Fig. 2) during the outburst had spectral index  $\alpha = 0.68$  and flux parameter  $F'_0 = 5.76 \times 10^{-5} \text{ s}^{-1} \text{ cm}^{-2}$  (note that the flux given by their eq. [1] appears too large by a factor of 10). For this value of  $\alpha$ , we obtain  $y = 1.6$  (see eq. [2.1]) and  $\Psi(\alpha) = 0.245$  (see Fig. 1), and for the redshift of 3C 279 ( $\mathcal{Z} = 0.538$ ), we obtain the luminosity distance (Lang 1980)  $D = H_0^{-1} c [\mathcal{Z} + 0.5(1 - q_0)\mathcal{Z}^2] = 5.65 \times 10^{27} \text{ cm}$  assuming  $q_0 = 0.5$  and  $H_0 = 100 \text{ km s}^{-1} \text{ Mpc}^{-1}$ . We can relate  $F'_0$  to the disk-frame intensity parameter  $I_0$  using

$$I_0 = \frac{(2 - \omega)(1 + \mathcal{Z})^{3+\alpha} F'_0}{2\pi} \left( \frac{D}{R_g} \right)^2 \left[ \left( \frac{R_0}{R_g} \right)^{2-\omega} - \left( \frac{R_{ms}}{R_g} \right)^{2-\omega} \right]^{-1}, \quad (5.1)$$

according to equations (2.8) and (2.9).

## 5.1. Distance to the Gamma-Ray Emission Site

As an application, we consider first the simplest geometrical case, that of a  $\gamma$ -ray propagating away from the black hole along the axis of a two-temperature disk emitting with the power-law X-ray intensity given by equation (2.3). This scenario is useful for determining the minimum height above the disk at which the observed  $\gamma$ -radiation could have been produced in 3C 279 in 1991

June. We can calculate the optical depth to pair production for a  $\gamma$ -ray of energy  $E$  created at height  $z$  above the center of the disk and propagating outward along the  $z$ -axis using equation (4.3). In order to calculate  $\tau_{\gamma\gamma}$ , we must assume values for the inner ( $R_{\text{ms}}$ ) and outer ( $R_0$ ) radii of the two-temperature, X-ray-emitting region. In Figure 3 we set  $R_{\text{ms}} = 6R_g$  (accretion onto a Schwarzschild black hole) and  $R_0 = 30R_g$  (a typical value for the outer radius; see SLE and EK), and plot  $\log \tau_{\gamma\gamma}$  as a function of  $\log(M/M_\odot)$  and  $\log(z/R_g)$  for a  $\gamma$ -ray of energy  $E = 1$  GeV using the X-ray data taken during the 1991 June EGRET flare of 3C 279. The optical depth exceeds unity in the cross-hatched area, and  $\tau_{\gamma\gamma} = 1$  along the heavy solid line denoting the  $\gamma$ -ray photosphere, with height  $z = z_{\gamma\gamma}$ . For reference,  $z = R_0$  along the upper dashed horizontal line, and  $z = R_{\text{ms}}$  along the lower dashed line. The slope of the contours depends on how close to the disk the  $\gamma$ -rays are produced relative to  $R_{\text{ms}}$  and  $R_0$ . For  $z \lesssim R_{\text{ms}}$ , the contours become increasingly vertical because the absorption coefficient loses its dependence on  $z$  close to the disk. For  $z \gtrsim R_0$ , the contours make a transition to the far-field power-law behavior given by equation (4.6), which reduces to  $\tau_{\gamma\gamma} \cong 2.4 \times 10^{16} (M/M_\odot)^{-1} (z/R_g)^{-4.36}$  for the parameters used in Figure 3.

In the case of 3C 279, we find that when  $M \gtrsim 4 \times 10^{11} M_\odot$ , the intensity is so low that  $\tau_{\gamma\gamma} < 1$  regardless of the value of  $z$ . On the other hand, we see that observable  $\gamma$ -rays can be produced quite close to the black hole for reasonable values of  $M$  if  $z \gtrsim R_0$ . For example, if  $M = 10^9 M_\odot$ , then  $\tau_{\gamma\gamma} < 1$  for  $z > z_{\gamma\gamma} = 45R_g = 2 \times 10^{-3}$  pc. This suggests that  $\gamma$ -rays produced at the top of the evacuated funnel at the center of a hot accretion disk (perhaps as a consequence of MHD waves generated in the surrounding hot-disk plasma; see Becker & Kafatos 1994) can escape without  $\gamma - \gamma$  attenuation by the disk X-rays (although they may suffer attenuation by scattered X-rays on larger spatial scales; see Dermer & Schlickeiser 1994).

The precise value of the outer radius  $R_0$  of the two-temperature region is uncertain, but it is likely to fall in the range  $30 \lesssim R_0/R_g \lesssim 100$  (SLE; EK). In Figure 4 we therefore recompute the  $\tau_{\gamma\gamma}$  contours using the same parameters as in Figure 3, except  $R_0 = 100R_g$ . Here again  $z = R_0$  and  $z = R_{\text{ms}}$  along the upper and lower dashed lines, respectively. The differences between Figures 3 and 4 are not dramatic, although the height of the  $\gamma$ -ray photosphere has increased from  $z_{\gamma\gamma} = 45R_g$  to  $z_{\gamma\gamma} = 70R_g$  for  $M = 10^9 M_\odot$ . This is due to the presence of X-ray photons emitted at large radii, for which the interaction angle  $\theta$  (and therefore the probability of pair production) is enhanced. In this case, equation (4.6) for the approximate far-field solution reduces to  $\tau_{\gamma\gamma} \cong 3.6 \times 10^{17} (M/M_\odot)^{-1} (z/R_g)^{-4.36}$ , in good agreement with Figure 4 for  $z \gtrsim R_0$ .

To investigate the effect of the angular dependence of the  $\gamma - \gamma$  absorption coefficient on the values obtained for  $\tau_{\gamma\gamma}$ , in Figure 5 we plot the height of the  $\gamma$ -ray photosphere,  $z_{\gamma\gamma}/R_g$ , as a function of the black hole mass  $M/M_\odot$  for  $R_{\text{ms}} = 6R_g$  and  $\omega = 0$  (uniformly bright disk; *dashed line*) or  $\omega = 3$  (two-temperature disk; *solid line*). We compare results obtained using our two standard values for the outer radius,  $R_0 = 30R_g$  (*open squares*) and  $R_0 = 100R_g$  (*open triangles*). When  $\omega = 3$ , increasing  $R_0$  from  $30R_g$  to  $100R_g$  causes only a modest increase in the height of the photosphere as mentioned above. However, going from  $\omega = 3$  to  $\omega = 0$  while holding  $R_0$  constant results in a substantial increase in  $z_{\gamma\gamma}$  due to the increased amount of X-radiation impinging on the axially propagating  $\gamma$ -rays from large radii, where the interaction angle  $\theta$  has its maximum value. This effect is particularly strong for  $R_0 = 100R_g$ .

It is also interesting to consider the effect of varying the inner radius of the disk,  $R_{\text{ms}}$ , since this will also impact on the angular distribution of the X-rays. In Figure 6 we plot the photosphere height  $z_{\gamma\gamma}/R_g$  as a function of  $M/M_\odot$  for  $R_{\text{ms}}/R_g = 2$ ,  $R_0/R_g = (30, 100)$ , and  $\omega = (0, 3)$ . These results may represent approximately situations involving disks around Kerr black holes, for which the radius of marginal stability can approach  $1.2R_g$  (Shapiro & Teukolsky 1983). In this case equation (2.2) for the flux  $F(R)$  is no

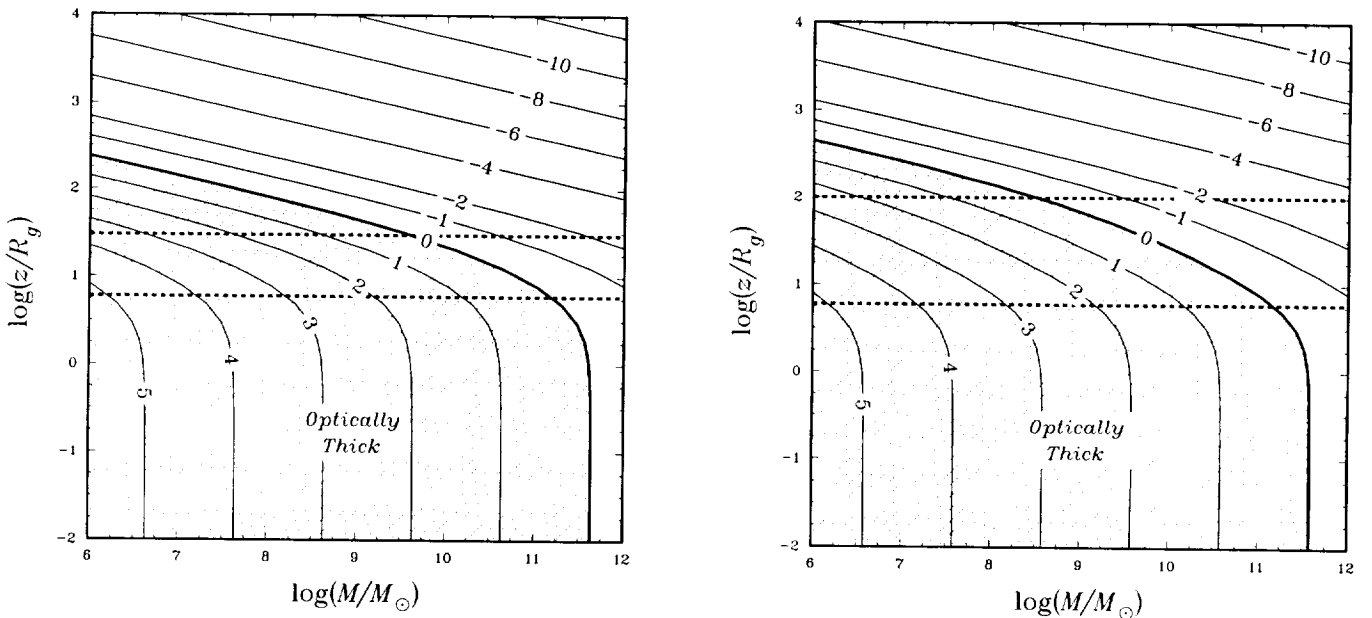


FIG. 3.—Contour plot of the log of the  $\gamma - \gamma$  optical depth  $\tau_{\gamma\gamma}$  (eq. [4.3]) for  $\gamma$ -rays with energy  $E = 1$  GeV created at height  $z$  above the center of a two-temperature disk ( $\omega = 3$ ) with outer radius  $R_0 = 30R_g$  and inner radius  $R_{\text{ms}} = 6R_g$ . The upper and lower dashed horizontal lines denote  $z = R_0$  and  $z = R_{\text{ms}}$ , respectively, and the  $\gamma$ -rays propagate outward along the  $z$ -axis. The curves were computed using the X-ray data for 3C 279 taken during the 1991 June EGRET flare by Makino et al. (1993).

FIG. 4.—Same as Fig. 3, except  $R_0 = 100R_g$ .

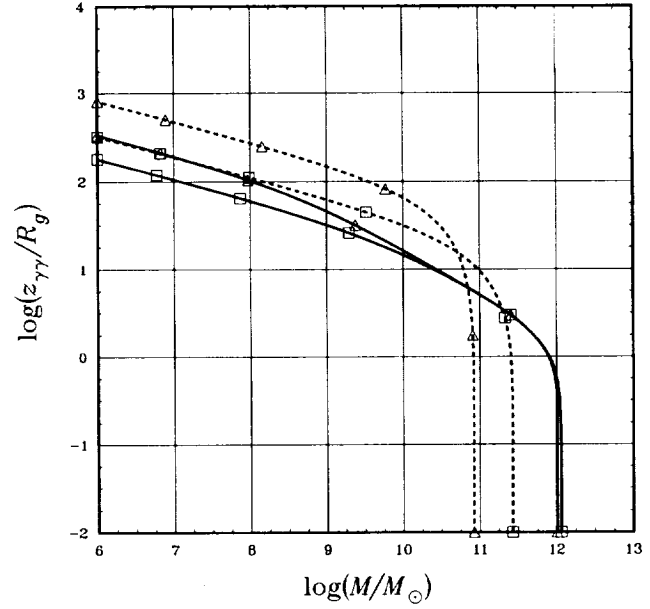
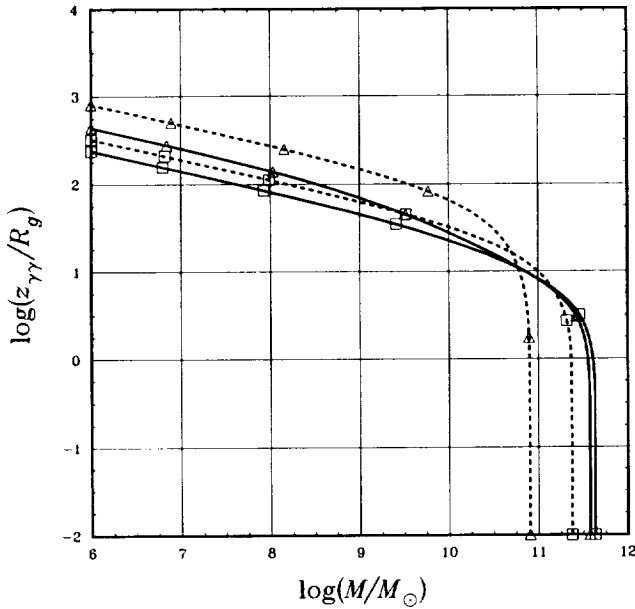


FIG. 5.—Height of the  $\gamma$ -ray photosphere,  $z_{\gamma\gamma}/R_g$ , plotted as a function of the black hole mass  $M/M_\odot$  for  $R_{ms} = 6R_g$  and  $\omega = 0$  (dashed line),  $\omega = 3$  (solid line),  $R_0 = 30R_g$  (open squares),  $R_0 = 100R_g$  (open triangles). The curves were computed using the 1991 June 3C 279 X-ray data.  
 FIG. 6.—Same as Fig. 5, except  $R_{ms} = 2R_g$

longer valid, although the flux still maintains the approximate power-law radial dependence  $F(R) \propto R^{-3}$  (Eilek 1980). Obviously our model cannot be rigorously defended in this context since we have completely neglected relativistic effects, but, bearing this caveat in mind, it is interesting to note the modest decrease in the height of the photosphere going from Figure 5 to Figure 6 when  $\omega = 3$ , due to the decrease in the flux-averaged value of the interaction angle  $\theta$ . By contrast, the results depicted in Figures 5 and 6 agree closely when  $\omega = 0$  (uniformly bright disk), because then most of the emission comes from radii  $R \gg R_{ms}$ , and the value of  $R_{ms}$  is therefore irrelevant.

In Table 1 we give values for the height of the  $\gamma$ -ray photosphere  $z_{\gamma\gamma}/R_g$ , along with values for the associated light-crossing timescale (which may approximate the variability timescale),  $t_{\gamma\gamma} \equiv z_{\gamma\gamma}/c$ , for  $E = 1$  GeV,  $\omega = 3$ , and various values of the black hole mass  $M/M_\odot$ , the outer disk radius  $R_0/R_g$ , and the inner disk radius  $R_{ms}/R_g$ . Table 1 also includes values for the disk-frame intensity parameter  $I_0$ . Using our standard parameters  $M = 10^9 M_\odot$ ,  $R_0 = 30R_g$ ,  $R_{ms} = 6R_g$ , and  $\omega = 3$ , we find that  $t_{\gamma\gamma} \sim 2$  days, in agreement with the  $\gamma$ -ray variability timescale reported by Kniffen et al. (1993).

5.2. Gamma-Ray Collimation

The dependence of the  $\gamma - \gamma$  absorption probability on the angular distribution of the X-rays suggests that pair production may help to collimate the high-energy radiation escaping from blazars. We expect that for given values of the inner and outer disk radii  $R_{ms}$  and  $R_0$ , the optical depth to pair production for  $\gamma$ -rays originating at a fixed location above the center of the disk will increase with increasing propagation angle  $\Phi$ , mainly due to an increase in the flux-averaged value of the interaction angle  $\theta$ , and to a lesser extent because the  $\gamma$ -rays remain close to the disk for a longer period of time. We shall continue to work with X-ray data obtained during the 1991 June flare of 3C 279 in all of the examples.

TABLE 1  
 MODEL RESULTS FOR 3C 279

$M$ ( $M_\odot$ )	$R_0$ ( $R_g$ )	$R_{ms}$ ( $R_g$ )	$z_{\gamma\gamma}$ ( $R_g$ )	$t_{\gamma\gamma}$ (d)	$\Delta\Phi$ (deg)	$I_0$ ( $s^{-1} \text{ cm}^{-2} \text{ sr}^{-1}$ )
$10^8$ .....	30	6	81.2	0.46	5.7	$4.9 \times 10^{25}$
	30	2	59.9	0.34	6.0	$1.4 \times 10^{25}$
	100	6	141.2	0.81	7.8	$4.2 \times 10^{25}$
$10^9$ .....	30	2	101.8	0.58	7.7	$1.3 \times 10^{25}$
	30	6	45.2	2.57	9.5	$4.9 \times 10^{23}$
	100	2	32.0	1.82	9.7	$1.4 \times 10^{23}$
$10^{10}$ .....	30	6	69.9	3.98	12.1	$4.2 \times 10^{23}$
	30	2	45.9	2.62	11.6	$1.3 \times 10^{23}$
	100	6	22.5	12.85	15.3	$4.9 \times 10^{21}$
	30	2	14.6	8.31	14.6	$1.4 \times 10^{21}$
	100	6	27.6	15.74	17.2	$4.2 \times 10^{21}$
	100	2	16.3	9.31	15.4	$1.3 \times 10^{21}$

We can use equation (4.1) to calculate the optical depth  $\tau_{\gamma\gamma}$  for  $\gamma$ -rays of energy  $E$  created at a height  $z$  above the center of the disk and propagating at an angle  $\Phi$  with respect to the  $z$ -axis. In order to explore the angular dependence of  $\gamma - \gamma$  attenuation, in Figures 7 and 8 we plot the transmission coefficient  $\exp(-\tau_{\gamma\gamma})$  calculated using the 3C 279 X-ray data as a function of  $\Phi$  for  $R_{\text{ms}} = 6R_g$ ,  $E = 1$  GeV,  $M = 10^9 M_\odot$ , and various values of  $R_0$  and  $z$ . The transmission coefficient gives the fraction of the  $\gamma$ -rays that would escape to infinity in a given direction out of those emitted in that direction. We set  $R_0 = 30R_g$  in Figure 7,  $R_0 = 100R_g$  in Figure 8, and, to illustrate the importance of angular effects, we set  $\omega = 3$  in Figures 7a and 8a, and  $\omega = 0$  in Figures 7b and 8b. Strong "focusing" of the escaping  $\gamma$ -rays along the  $z$ -axis is apparent in all cases, and, for  $\omega = 3$ , the half-width of the angular distribution,  $\Delta\Phi$ , falls in the range  $10^\circ \lesssim \Delta\Phi \lesssim 20^\circ$ . Similar results are obtained for  $\Delta\Phi$  when  $\omega = 0$  (Figs. 7b and 8b), but the overall level of attenuation is much greater in these cases due to the enhancement of the X-ray emission produced at large radii in the disk. In Table 1 we give values for  $\Delta\Phi$  evaluated at the photosphere,  $z = z_{\gamma\gamma}$ , for various model parameters. Our results for  $\Delta\Phi$  are comparable to the observationally determined values (e.g., Padovani & Urry 1992), and we therefore conclude that for acceptable disk parameters,  $\gamma - \gamma$  attenuation alone is enough to produce the degree of  $\gamma$ -ray collimation implied by observations which associate extragalactic  $\gamma$ -ray emission with blazars.

### 5.3. Shape of the Gamma-Ray Photosphere

The high-energy  $\gamma$ -rays observed from many blazars are emitted nearly parallel to the axis of the jet, as is evidenced particularly by the common occurrence of apparent superluminal motion in the sources. It is therefore interesting to calculate, within the context of our model, the  $\gamma - \gamma$  optical depth for a  $\gamma$ -ray created at radius  $R$  and height  $z$ , and subsequently propagating parallel to the  $z$ -axis of the disk, which can be obtained by setting  $\Phi = 0$  in equation (4.1). It is particularly interesting to determine the shape of the  $\gamma$ -ray photosphere by varying the value of the  $\gamma$ -ray creation radius  $R$ .

In Figure 9, we plot the photosphere height  $z_{\gamma\gamma}/R_g$  calculated using the 3C 279 X-ray data as a function of  $R/R_g$  for various values of  $M/M_\odot$ , assuming our standard parameters  $R_0 = 30R_g$ ,  $R_{\text{ms}} = 6R_g$ , and  $\omega = 3$ . We find that the height of the photosphere increases dramatically as  $M$  decreases, and the shape of the photosphere becomes quite concave. Conversely, for large values of  $M$ , the photosphere becomes nearly flat. We interpret this behavior as follows. For large values of  $M$ , the disk-frame intensity parameter  $I_0$  is small, and therefore the photosphere is located relatively close to the disk, with  $z_{\gamma\gamma}/R_0 \lesssim 1$ . In this case, most of the  $\gamma - \gamma$  absorption takes place so close to the disk that the flux-averaged value of the interaction angle  $\theta$  is nearly  $90^\circ$  at all points in the photosphere, and therefore the height of the photosphere varies little across the disk. On the other hand, as  $M$  decreases,  $I_0$  becomes large, and consequently the photosphere lies farther from the disk, with  $z_{\gamma\gamma}/R_0 \gtrsim 1$ . In this case, the flux-averaged value of  $\theta$  increases significantly going from the center of the photosphere to the edge, and therefore the height of the photosphere must increase rapidly in order to keep  $\tau_{\gamma\gamma} = 1$ , as seen in Figure 9.

## 6. DISCUSSION

Although the physics of particle creation and acceleration far from the turbulent plasma accreting onto a black hole is poorly understood, there are a number of relatively well-understood plasma and accretion instabilities that can give rise to efficient particle

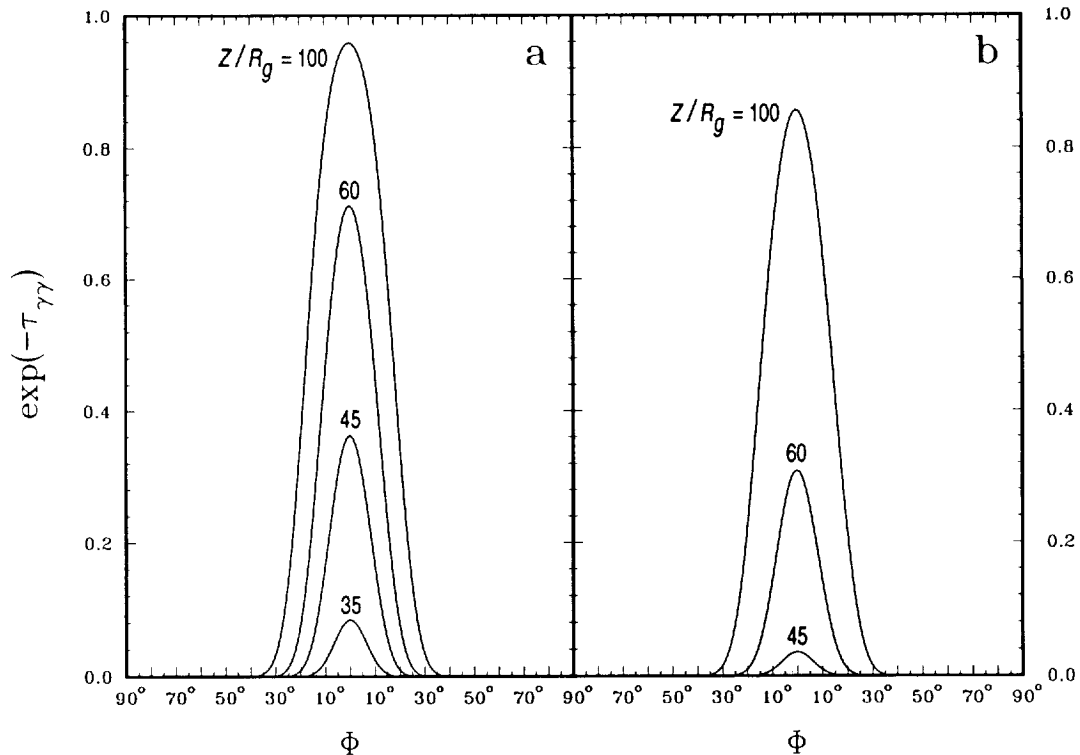


FIG. 7.—Transmission coefficient  $\exp(-\tau_{\gamma\gamma})$  plotted as a function of the propagation angle  $\Phi$  using the 1991 June 3C 279 X-ray data for  $M = 10^9 M_\odot$ ,  $R_0 = 30R_g$ ,  $R_{\text{ms}} = 6R_g$  and (a)  $\omega = 3$ , (b)  $\omega = 0$ . The  $\gamma$ -rays are created at the height  $z/R_g$  indicated for each curve.

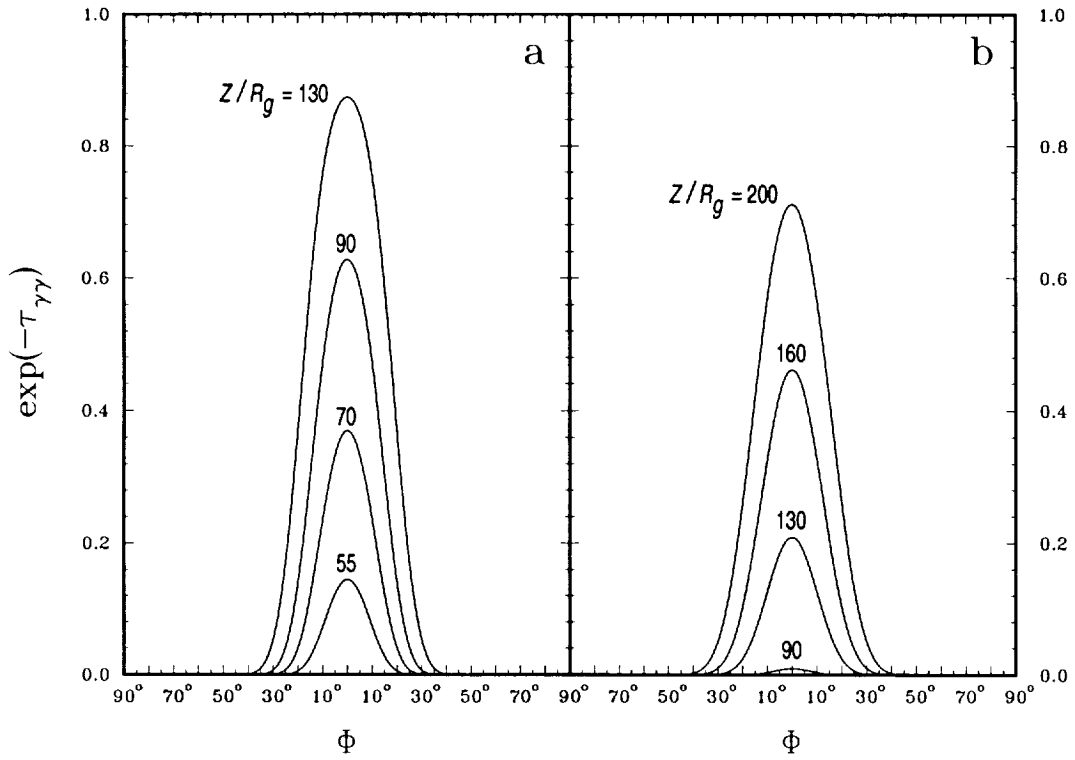


FIG. 8.—Same as Fig. 7, except  $R_0 = 100R_g$

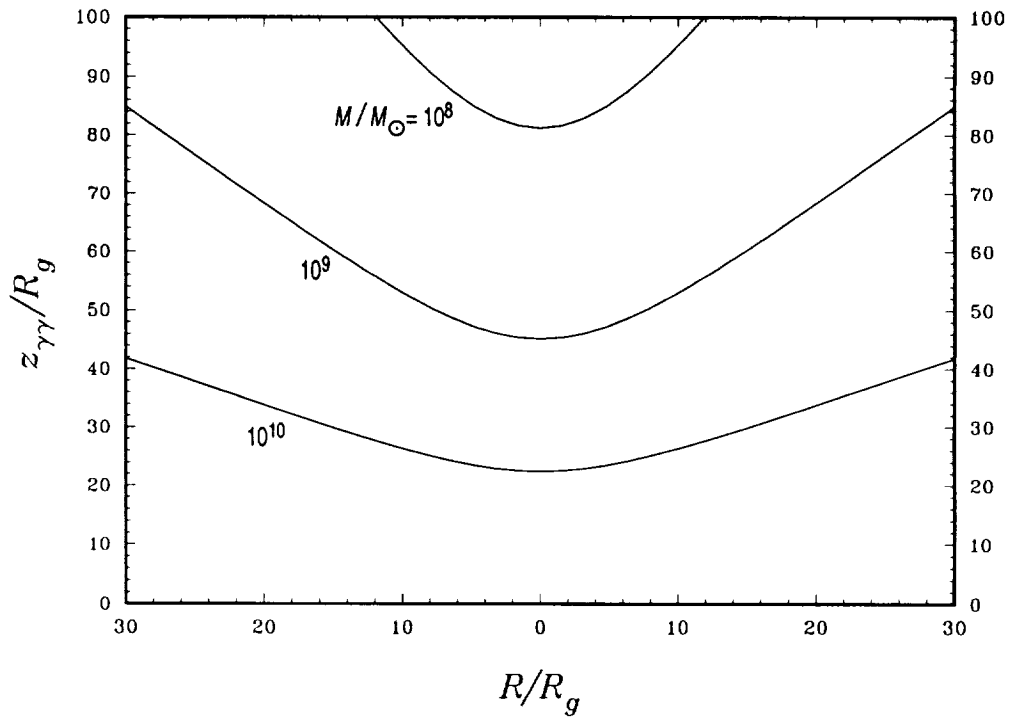


FIG. 9.—Height of the  $\gamma$ -ray photosphere  $z_{\gamma}/R_g$  plotted as a function of the creation radius  $R/R_g$  for  $\gamma$ -rays propagating parallel to the  $z$ -axis using the 1991 June 3C 279 X-ray data, assuming  $R_0 = 30R_g$ ,  $R_{ms} = 6R_g$ , and  $\omega = 3$ . The value of the black hole mass  $M/M_{\odot}$  is indicated for each curve.

acceleration within the disk itself, or within the evacuated funnel region at the center of the disk. For example, resonant turbulent acceleration via interactions between particles and (linear or nonlinear) Alfvén waves can in principle lead to the production of electrons with very high Lorentz factors, and to the associated emission of high-energy inverse-Compton  $\gamma$ -rays (e.g., Becker & Kafatos 1994; Becker et al. 1994). However, in order for any of these mechanisms to create *observable*  $\gamma$ -rays, the optical depth to pair production on the background UV and X-ray photons must be small enough for the  $\gamma$ -rays to escape from the source.

In this paper, we have attempted to bridge the gap between theory and observation by developing useful constraints based on the simple hypothesis that the power-law X-ray spectrum originates in the inner region of a two-temperature accretion disk. Such disks commonly provide good fits to the hard X-ray spectra of AGNs. In § 3 we developed a general expression for the  $\gamma - \gamma$  absorption coefficient  $\alpha_{\gamma\gamma}$  for  $\gamma$ -rays propagating above a two-temperature disk in a plane that includes the symmetry axis, and in § 4 we derived an approximate far-field solution for the  $\gamma - \gamma$  optical depth  $\tau_{\gamma\gamma}$  for  $\gamma$ -rays created above the center of the disk and propagating outward along the disk axis, taking full account of the angular dependence of the X-ray distribution. In § 5 we applied our results to 3C 279 using the X-ray data reported by Makino et al. (1993) during the 1991 June  $\gamma$ -ray flare, and demonstrated that the observed  $\gamma$ -rays could have been produced within  $\lesssim 45GM/c^2$  of a black hole of mass  $M \gtrsim 10^9 M_\odot$ . This is close enough to the central source to establish a direct connection between the production of the  $\gamma$ -rays and the accretion of material onto the black hole. In particular, our results suggest that the observed  $\gamma$ -rays may have been produced near the top of the evacuated funnel at the center of a hot, two-temperature accretion disk. In this scenario, the relativistic electrons that Compton-upscatter UV photons to produce the  $\gamma$ -rays are themselves produced as a consequence of photon-photon collisions in the funnel. The absence of protons in the funnel due to the centrifugal barrier allows the presence of Alfvén waves with wavelengths short enough to effectively accelerate the electrons (Becker et al. 1994).

In order to explore the observational implications of the angular dependence of  $\gamma - \gamma$  pair production, in § 5 we also computed  $\tau_{\gamma\gamma}$  for  $\gamma$ -rays born along the disk axis but propagating at an angle  $\Phi$  with respect to it. The results for the half-angle ( $\Delta\Phi \lesssim 15^\circ$ ) indicated in Figures 7 and 8 and in Table 1 suggest that pair production in the X-ray field of the accretion disk may be strong enough to explain the observed degree of  $\gamma$ -ray alignment in blazars. Furthermore, the variability (light-crossing) timescale  $t_{\gamma\gamma} \equiv z_{\gamma\gamma}/c$  we derive for black hole mass  $M \sim 10^9 M_\odot$  is in good agreement with the 2-day  $\gamma$ -ray variability of 3C 279 reported by Kniffen et al. (1993).

The results presented in §§ 4 and 5 suggest that  $\gamma - \gamma$  pair production can help to “focus” an intrinsically isotropic source of  $\gamma$ -rays so that the high-energy radiation escapes preferentially along the disk axis. Whether or not the  $\gamma$ -rays actually are produced isotropically is a separate question. If they are, then several additional considerations come into play, regarding (i) the self-opacity of the  $\gamma$ -rays; (ii) the fate of the  $\gamma$ -ray energy emitted off-axis; and (iii) the required total luminosity.

### 6.1. $\gamma - \gamma$ Self-Opacity

Whether or not the high-energy  $\gamma$ -rays are produced by an intrinsically isotropic source, their self-interaction optical depth  $\tau_{\text{self}}$  cannot exceed unity if they are to be observed. The most severe self-interaction constraint is obtained in the case of isotropic emission. Assuming a monochromatic, isotropic distribution of  $\gamma$ -rays with energy  $E_0 > m_e c^2$  and intensity  $I_\epsilon = B\delta(E - E_0)$ , integration of equation (3.3) yields for the self-interaction absorption coefficient

$$\alpha_{\text{self}} = \frac{8\pi B}{cE} \left( \frac{E}{m_e c^2} \right)^{-4} \int_0^{\beta_{\text{max}}} \sigma_{\gamma\gamma}(\beta) \frac{2\beta d\beta}{(1 - \beta^2)^3}, \quad (6.1)$$

where  $\sigma_{\gamma\gamma}(\beta)$  is given by equation (3.1) and

$$\beta_{\text{max}} = \left[ 1 - \left( \frac{E}{m_e c^2} \right)^{-2} \right]^{1/2}. \quad (6.2)$$

If the  $\gamma$ -ray source is an isotropically emitting sphere of radius  $R_*$ , then the intensity parameter  $B$  is related to the  $\gamma$ -ray luminosity  $L_\gamma$  via

$$B = \frac{L_\gamma}{(2\pi R_*)^2}, \quad (6.3)$$

and we obtain for the self-interaction  $\gamma - \gamma$  optical depth

$$\tau_{\text{self}} \equiv R_* \alpha_{\text{self}} = \frac{2L_\gamma \sigma_T}{\pi R_* cE} \left[ \left( \frac{E}{m_e c^2} \right)^{-4} \int_0^{\beta_{\text{max}}} \frac{\sigma_{\gamma\gamma}(\beta)}{\sigma_T} \frac{2\beta d\beta}{(1 - \beta^2)^3} \right]. \quad (6.4)$$

An isotropic  $\gamma$ -ray source can be ruled out if  $\tau_{\text{self}}$  exceeds unity for reasonable values of  $R_*$ . The first factor on the right-hand side of equation (6.4) is essentially the standard  $\gamma$ -ray compactness, and the quantity in brackets becomes  $\sim 10^{-6}$  for  $E = 1$  GeV. Taking  $L_\gamma = 10^{48}$  ergs  $s^{-1}$  for 3C 279 and setting  $\tau_{\text{self}} < 1$  yields the easily satisfied transparency requirement  $R_* \gtrsim 10^{10}$  cm, and therefore self-interaction of the GeV radiation in 3C 279 is not likely to be important. A similar calculation by McNaron-Brown et al. (1995) indicates that the self-interaction of radiation in the energy range 0.05–10 MeV (observed by OSSE) is also negligible.

### 6.2. Fate of the Off-Axis Radiation

If the  $\gamma$ -rays are produced isotropically, then only those emitted close to the disk axis will escape from the X-ray field of the accretion disk. The radiation emitted farther from the axis will be degraded in a pair-Compton cascade (Protheroe, Mastichiadis, & Dermer 1992), with most of the luminosity residing ultimately in a broad MeV feature. In this view, objects such as 3C 279 (while in

$\gamma$ -ray flare mode) will appear as bright sources of MeV emission when viewed along lines of sight  $\gtrsim 20^\circ$  from the disk axis. Centaurus A may be an example of such an object (Skibo, Dermer, & Kinzer 1995).

The luminosity required to power isotropic  $\gamma$ -ray emission,  $L_\gamma = 10^{48}$  ergs  $s^{-1}$ , is orders of magnitude higher than that required if the emission is beamed. This is perhaps the simplest argument against isotropic emission, but it is especially compelling when coupled with the strong circumstantial evidence in favor of relativistic bulk motion. However, there is apparently no strong a priori reason to rule out isotropic emission, since attenuation due to collisions with X-rays emitted by the disk is sufficient to produce the observed degree of alignment. In any event, our results regarding  $\gamma - \gamma$  collimation do not rely on the existence of an isotropic  $\gamma$ -ray source. The mechanism we consider here can work in concert with other sources of collimation, such as relativistic bulk motion or geometrical focusing.

### 6.3. Attenuation by Scattered X-Rays

The backscattering of X-rays produced in the accretion disk by electrons located above the disk tends to isotropize the X-ray distribution, and this can have a strong effect on the results obtained for the  $\gamma - \gamma$  absorption coefficient. We believe that our neglect of a scattered component to the X-ray distribution is reasonable due to the proximity of the  $\gamma$ -ray production site to the black hole in our model. It has been shown (Dermer & Schlickeiser 1994) that accretion disk photons will dominate over scattered X-rays within a distance of  $\sim 0.01$ – $0.1$  pc from the central source, which is much larger than the typical height of the  $\gamma$ -ray photosphere,  $z_{\gamma\gamma}$ , obtained here (see Table 1). However, the problem of  $\gamma - \gamma$  attenuation by scattered X-rays on much larger spatial scales is a serious issue that must be addressed using detailed calculations that determine self-consistently the angle and energy distributions of both the scattered radiation and the electron-positron pairs at large distances from the black hole. Such a calculation is beyond the scope of this paper, but it suggests a promising direction for future work.

Our results indicate that if the emission height  $z$  is held fixed, then the optical depth increases with increasing  $\gamma$ -ray energy  $E$  as  $\tau_{\gamma\gamma} \propto E^\alpha$ , and therefore the height of the  $\gamma$ -ray photosphere  $z_{\gamma\gamma}$  increases with increasing  $E$ . If we arbitrarily set the emission height for all of the  $\gamma$ -rays equal to the value of  $z_{\gamma\gamma}$  obtained for  $E = 1$  GeV, then the observed spectrum will be attenuated by a factor  $\sim 7$  going from  $E = 1$  GeV to  $E = 5$  GeV. It is unclear whether such a steepening actually exists in the spectrum of 3C 279 (Hartman et al. 1992). Finally, for energies  $E \gtrsim 5$  GeV, the interaction with UV radiation produced in the cool outer region of the disk may become important, further raising the height of the photosphere.

To summarize our main points, application of our general expressions describing  $\gamma - \gamma$  attenuation above X-ray-emitting accretion disks leads us to conclude that in the case of 3C 279, (i)  $\gamma$ -ray transparency (to disk-generated X-rays) is achieved if the  $\gamma$ -rays are produced at height  $z \gtrsim R_0$ ; (ii)  $\gamma - \gamma$  attenuation is strong enough to explain the observed association of high-energy  $\gamma$ -ray emission from AGNs exclusively with blazars; and (iii) the observed  $\gamma$ -rays may be produced in active plasma located above the funnel at the center of a two-temperature accretion disk.

We gratefully acknowledge the remarks provided by the anonymous referee, whose insightful comments contributed significantly to the paper. This work was partially supported by a NASA Cycle 3 *CGRO* Guest Investigator grant.

### REFERENCES

- Becker, P. A., & Kafatos, M. 1994, in *The Second Compton Symp.*, ed. C. E. Fichtel, N. Gehrels, & J. P. Norris (New York: AIP), 620  
 Becker, P. A., Kafatos, M., & Maisack, M. 1994, *ApJS*, 90, 949  
 Bednarek, W. 1993, *A&A*, 278, 307  
 Begelman, M. C., Blandford, R. D., & Rees, M. J. 1984, *Rev. Mod. Phys.*, 56, 255  
 Blandford, R. D. 1993, in *Proc. Compton Gamma-Ray Observatory Symp.*, ed. M. Friedlander, N. Gehrels, & D. J. Macomb (New York: AIP), 533  
 Dermer, C. D., & Schlickeiser, R. 1993, *ApJ*, 416, 458  
 ———. 1994, *ApJS*, 90, 945  
 Eilek, J. A. 1980, *ApJ*, 236, 664  
 Eilek, J. A., & Kafatos, M. 1983, *ApJ*, 271, 804 (EK)  
 Fichtel, C. E., et al. 1994, *The First Energetic Gamma-Ray Experiment Telescope (EGRET) Source Catalog* (Washington, DC: NASA)  
 Gould, R. J., & Schröder, G. P. 1967, *Phys. Rev.*, 155, 1404  
 Hartman, R. C., et al. 1992, *ApJ*, 385, L1  
 Hermsen, W., et al. 1993, *A&AS*, 97, 97  
 Jauch, J. M., & Rohrlich, F. 1955, *Theory of Photons and Electrons* (Reading: Addison-Wesley)  
 Kniffen, D. A., et al. 1993, *ApJ*, 411, 133  
 Lang, K. R. 1980, *Astrophysical Formulae* (New York: Springer)  
 Makino, F., et al. 1989, *ApJ*, 347, L9  
 Makino, F., et al. 1993, in *Frontiers of Neutrino Astrophysics*, ed. Y. Suzuki & K. Nakamura (Tokyo: Universal Press), 425  
 McNaron-Brown, K., et al. 1994, in *The Second Compton Symp.*, ed. C. E. Fichtel, N. Gehrels, & J. P. Norris (New York: AIP), 587  
 McNaron-Brown, K., et al. 1995, *ApJ*, 451, 575  
 Padovani, P., & Urry, C. M. 1992, *ApJ*, 387, 449  
 Pringle, J. E. 1981, *ARA&A*, 19, 137  
 Protheroe, R. J., Mastichiadis, A., & Dermer, C. D. 1992, *Astroparticle Phys.*, 1, 113  
 Shakura, N. I., & Sunyaev, R. A. 1973, *A&A*, 24, 337  
 Shapiro, S. L., Lightman, A. P., & Eardley, D. M. 1976, *ApJ*, 204, 187 (SLE)  
 Shapiro, S. L., & Teukolsky, S. A. 1983, *Black Holes, White Dwarfs, and Neutron Stars* (New York: Wiley)  
 Skibo, J. G., Dermer, C. D., & Kinzer, R. L. 1995, *ApJ*, in press  
 von Montigny, C., et al. 1995, *ApJ*, 440, 525